Short-range-order effects on the ESR spectra of a spin cluster

Alzira M. Stein and G. G. Cabrera
Instituto de Física "Gleb Wataghin," Universidade Estadual de Campinas, 13100-Campinas, Sao Paulo, Brazil

L. M. Falicov
Department of Physics, University of California, Berkeley, California 94720

(Received 17 November 1980)

Using the Kikuchi counting for the Ising problem, we present a theory which takes into account short-range-order effects in the formation of spin clusters. The Weiss molecular-field treatment is thus improved, since partial spin alignment is allowed in the paramagnetic phase. The above approach is used to study the influence of short-range order on the electron-spin-resonance (ESR) spectra of a spin system. Two main effects are then predicted: (i) One is related to a shift of resonances towards higher frequencies when the temperature is lowered. This effect is induced by effective local fields generated by short-range order. (ii) The other deals with multiple splitting of lines as a manifestation of transitions between states corresponding to different cluster configurations. These results are in good qualitative agreement with experiments.

I. INTRODUCTION

The widely used Weiss molecular-field theory of magnetism[1] describes a second-order phase transition where *no* correlations of spins are present in the paramagnetic (disordered) phase. The onset of the ordered phase (ferro- or antiferromagnetic) is accompanied by the production of long-range order and no fluctuations are allowed in the paramagnetic phase.

Still within the effective field theories, the Weiss molecular field treatment can be improved allowing partial spin alignments in the formation of clusters in the paramagnetic region.[1] A series of approximations, taking into account the short-range order, can be formulated.[1-3] From those, the method developed by Kikuchi[3] can be extended to successive orders of approximations as long as the order of multisite correlations is increased. The limiting cases of the single site and pair correlations correspond to the so-called Bragg-Williams and Bethe approximations, respectively. The Kikuchi approximation of counting for the entropy has recently been applied in a series of papers dealing with the theory of order-disorder in binary alloys.[4,5] We shall follow closely the approach of Ref. 5 in order to treat the Ising problem at the level of the Bethe approximation.

The gross features of the model are summarized below.

(a) The transition temperature (for both, the ferro- and antiferromagnetic cases) is lowered in relation to the molecular-field result (which in turn is an overestimation of T_c). The Bethe approximation yields

$$k_B T_c = \frac{2|J|}{\ln[Z/(Z-2)]} , \tag{1}$$

where Z is the number of nearest neighbors and J is the exchange constant. For $Z=2$ (linear chain) the result given by the model is exact and no phase transition is present. For $Z \geq 3$ we do obtain a phase transition but the result does not depend on the dimension or the crystalline structure employed. The only relevant parameter, apart from the exchange constant J, is Z, the number of nearest neighbors (called coordination number), and in some respects the approximation shows topological similarities with the linear chain (it can be pictured in the form of abstract structures called Cayley trees).

(b) The critical behavior, in the cases where we obtain a phase transition, is similar to that of the molecular field. A critical exponent $\beta = \frac{1}{2}$ is obtained for the magnetization.

(c) Short-range order is present in the paramagnetic phase in contrast with the molecular-field theory. This short-range order produces a tail in the specific heat as well as light deviations in the susceptibility[6] when compared with the Weiss model.

In this paper we want to describe some phenomena related to electron-spin resonance (ESR) which may be attributed to short-range-order correlations. Those effects include shifting of ESR resonances toward higher fields in the paramagnetic phase when the temperature is lowered toward the critical point, indicating the appearance of an internal field caused by coupling between neighboring spins.[7] Simultaneously with this effect, a multiple splitting of ESR lines has sometimes been observed[8] as a possible manifestation of clustering.

The theory developed in this paper explains qualitatively the phenomena mentioned above. The fer-

romagnetic and antiferromagnetic cases can be treated simultaneously by dividing the lattice into two equivalent and interpenetrating sublattices, which we shall call α and β. All the structures covered in this work are those where α sites have nearest neighbors of the β type only, and *vice versa* (as in the bcc structure).

In the next section the Kikuchi method is presented and the short-range and long-range parameters are calculated for both the ferromagnetic and antiferromagnetic cases when an external magnetic field is applied (as in a typical experiment of ESR). Whenever possible ($Z=4$) comparisons with Onsager's exact solution[9] are presented. The long-range-order parameters are identified with the sublattice magnetizations, while the short-range parameter is related to correlations of neighboring spins (and therefore is proportional to the internal energy per spin when only nearest-neighbor interactions are considered).

With the knowledge of the short- and long-range-order parameters, the site and bond probabilities are straightforwardly calculated. From this information the probabilities of formation of various clusters are inferred and the effective field at a given site can be computed as a function of temperature.

In Sec. III we show the resonant results for individual clusters and also the average case when superposition of the different clusters are considered. Whether individual clusters resonances can be observed in an actual experiment will depend on the experimental resolution.

In the last section we present the final comments and discuss the validity of our model. Since our method is an effective-field approach it will be no longer valid within the critical region. "Wrong" critical exponents are therefore predicted. It is worth remarking here that we are mainly interested in short-range-order properties which develop themselves in the paramagnetic phase far from the critical region. Classical molecular-field theory fails in describing such effects.

II. KIKUCHI APPROACH AND THE BETHE APPROXIMATION

As described in the Introduction we consider a lattice divided into two equivalent sublattices, α and β, and two states per site called A and B (spin up and down). All the nearest neighbors of an α site are of β type and *vice versa*.

We define the site probabilities p_K^ν as being the probability of finding a spin in the state K ($K=A,B$) at a site of the ν type ($\nu=\alpha,\beta$). We therefore end up with four site probabilities p_A^α, p_B^α, p_A^β, and p_B^β.

For the pair probabilities all the possibilities are listed in Fig. 1 along with the exchange energy for interacting pairs. For the structures considered here we

BOND	PROBABILITY	INTERACTION ENERGY
α β Ⓐ——Ⓐ	$p_{AA}^{\alpha\beta}$	J
Ⓐ——Ⓑ	$p_{AB}^{\alpha\beta}$	- J
Ⓑ——Ⓐ	$p_{BA}^{\alpha\beta}$	- J
Ⓑ——Ⓑ	$p_{BB}^{\alpha\beta}$	J

FIG. 1. The different bond configurations for the structures considered in this paper, where all the nearest neighbors of an α site are of the β type and *vice versa*. The pair exchange energy is also given along with the bond probabilities.

only get four bond probabilities denoted by $p_{AA}^{\alpha\beta}$, $p_{AB}^{\alpha\beta}$, $p_{BA}^{\alpha\beta}$, and $p_{BB}^{\alpha\beta}$.

Normalization requires the following constraints:

$$p_A^\alpha + p_B^\alpha = 1, p_A^\beta + p_B^\beta = 1 \ , \tag{2}$$

$$p_{AA}^{\alpha\beta} + p_{AB}^{\alpha\beta} + p_{BA}^{\alpha\beta} + p_{BB}^{\alpha\beta} = 1 \ , \tag{3}$$

$$p_{AA}^{\alpha\beta} + p_{BA}^{\alpha\beta} = p_A^\beta \ , \tag{4}$$

and

$$p_{BA}^{\alpha\beta} + p_{BB}^{\alpha\beta} = p_B^\alpha \ . \tag{5}$$

So we are left with only three independent parameters. We choose them as being two long-range order parameters (LROP)

$$M_\alpha \equiv p_A^\alpha - p_B^\alpha \ , \quad M_\beta \equiv p_B^\beta - p_A^\beta \ , \tag{6}$$

which can be identified with the sublattice magnetizations, and a short-range order parameter (SROP)

$$\eta \equiv p_{AA}^{\alpha\beta} + p_{BB}^{\alpha\beta} - p_{AB}^{\alpha\beta} - p_{BA}^{\alpha\beta} \ , \tag{7}$$

which corresponds to a correlation function between neighboring spins.

The Hamiltonian of our system is the usual Ising Hamiltonian with a Zeeman term

$$\mathcal{H} = J \sum_{\langle ij \rangle} \sigma_i \sigma_j - H \sum_i \sigma_i \ , \tag{8}$$

where the bracket $\langle ij \rangle$ means sum over nearest neighbors. The σ_i are operators which can take only the values $+1$ (corresponding to A) and -1 (corresponding to B). When $J=-|J|<0$ we get the ferromagnetic case, while antiferromagnetism is obtained for $J=|J|>0$.

With the use of diagrams from Fig. 1 and definition (7) the internal energy can be straightforwardly written as

$$E = \frac{ZN}{2} J (p_{AA}^{\alpha\beta} + p_{BB}^{\alpha\beta} - p_{AB}^{\alpha\beta} - p_{BA}^{\alpha\beta}) - NH\left(\frac{M_\alpha - M_\beta}{2}\right)$$

$$= \frac{ZN}{2} J\eta - NH\left(\frac{M_\alpha - M_\beta}{2}\right) \ . \tag{9}$$

Up to this point no approximation for the Ising problem has been made. The Kikuchi method[3] is an approximate counting of states for the entropy. Within the Bethe approximation Kikuchi's result is

$$S = NK_B \left[\frac{1}{2} \sum_{\nu=\alpha\beta} \sum_{K=A,B} (Z-1) p_K^\nu \ln p_K^\nu - \frac{1}{2} Z \sum_{K,L=A,B} p_{KL}^{\alpha\beta} \ln p_{KL}^{\alpha\beta} \right] . \quad (10)$$

Using the definitions (6) and (7) and the constraints (2)–(5) we can write the entropy in terms of parameters M_α, M_β, and η. The free energy

$$F(M_\alpha, M_\beta, \eta) = E - TS \quad (11)$$

is then minimized with respect to variations of those parameters, which yields the following transcendental conditions

$$\frac{p_{AA}^{\alpha\beta} p_{BB}^{\alpha\beta}}{p_{AB}^{\alpha\beta} p_{BA}^{\alpha\beta}} = e^{-4J/k_B T} , \quad (12)$$

$$\left[\frac{p_{AB}^{\alpha\beta}}{p_{BA}^{\alpha\beta}} \right]^Z = \left[\frac{p_A^\alpha p_B^\beta}{p_A^\beta p_B^\alpha} \right]^{Z-1} , \quad (13)$$

and

$$\left[\frac{p_A^\alpha p_A^\beta}{p_B^\alpha p_B^\beta} \right]^{Z-1} = e^{-4H/k_B T} \left[\frac{p_{AA}^{\alpha\beta}}{p_{BB}^{\alpha\beta}} \right]^Z . \quad (14)$$

The solutions provided by Eqs. (12)–(14) have the following general properties.

(i) For $Z=2$ and $H=0$ no phase transition is obtained. The SROP can be written in closed form

$$\eta = -\tanh(J/k_B T) , \quad (15)$$

which is the exact solution of the Ising model for the linear chain.

(ii) For the ferromagnetic case $J=-|J|<0$ and without external field ($H=0$) symmetry requires

$$M_\alpha = -M_\beta \equiv M \quad (16)$$

and

$$p_A^\alpha = p_A^\beta , \quad p_{AB}^{\alpha\beta} = p_{BA}^{\alpha\beta} . \quad (17)$$

Equation (13) is then a trivial identity and the magnetization M and the SROP η can be obtained numerically from the coupled relations (12) and (14). The transition temperature is given by relation (1).

(iii) In the antiferromagnetic case (with $H=0$), we have $J=|J|>0$ and also due to symmetry

$$M_\alpha = M_\beta = M . \quad (18)$$

The transition temperature is also given by relation (1). The symmetry condition (18) is no longer valid when an external magnetic field is applied.

(iv) For all cases the paramagnetic solution corresponds, within this approximation, to the linear-chain solution given by relation (15). This fact can be understood in terms of the topological similarities between Cayley trees and the linear chain.[10] For both structures only open trajectories are possible.

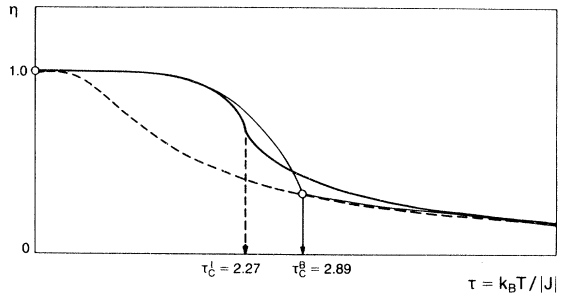

FIG. 2. The short-range order parameter (SROP) η as a function of the reduced temperature. We are showing here the $Z=4$ antiferromagnetic case (so what we are actually displaying is $-\eta=|\eta|$) in fine continuous line and comparing it with the exact Onsager solution for the two-dimensional case (thick continuous line). The paramagnetic solution is shown in dashed line and corresponds to the expression for the linear chain. The transition temperatures are indicated by arrows. Note that within the Bethe approximation the transition temperature is overestimated ($\tau_c^B=2.89$) and that the SROP has a discontinuous derivative at τ_c. The finite jump in the derivative is associated to a finite discontinuity of the specific heat at the critical point. In contrast, the exact solution displays a logarithmic singularity of the specific heat at the transition temperature. The Bethe solution (fine continuous line) and the linear-chain solution (dashed line) should coincide in the paramagnetic phase (they are slightly shifted in the figure for graphical purposes).

(v) The ferromagnetic linear chain with external field (along the spin direction) can be computed exactly and the results for the magnetization M and the parameter η are given in the Appendix.

In what follows we will use reduced variables defined by

$$\tau \equiv \frac{k_B T}{|J|} , \quad (19)$$

and

$$h \equiv \frac{H}{|J|} . \quad (20)$$

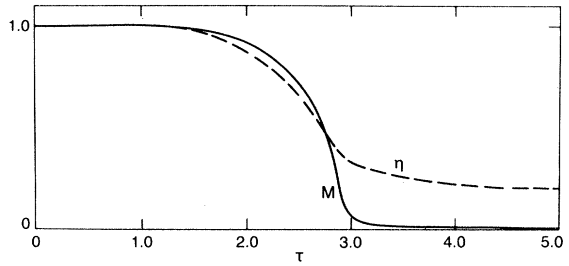

FIG. 3. The magnetization M for the ferromagnetic case, for $Z=4$ nearest neighbors, when an external magnetic field of magnitude $h=10^{-2}$ is applied. A smooth variation of parameters as functions of temperature is now obtained.

TABLE I. Cluster probabilities for $Z=4$ when the central site is of the α type. The effective field h_λ at the central site is also shown.

Nearest neighbors		h_λ	Probabilities
		Central spin: (A,α)	
A	B		
4	0	4	$p_A^\alpha (p_{AA}^{\alpha\beta}/p_A^\alpha)^4$
3	1	2	$4p_A^\alpha (p_{AB}^{\alpha\beta}/p_A^\alpha)(p_{AA}^{\alpha\beta}/p_A^\alpha)^3$
2	2	0	$6p_A^\alpha (p_{AB}^{\alpha\beta}/p_A^\alpha)^2(p_{AA}^{\alpha\beta}/p_A^\alpha)^2$
1	3	−2	$4p_A^\alpha (p_{AB}^{\alpha\beta}/p_A^\alpha)^3(p_{AA}^{\alpha\beta}/p_A^\alpha)$
0	4	−4	$p_A^\alpha (p_{AB}^{\alpha\beta}/p_A^\alpha)^4$
		Central spin: (B,α)	
0	4	−4	$p_B^\alpha (p_{BB}^{\alpha\beta}/p_B^\alpha)^4$
1	3	−2	$4p_B^\alpha (p_{BB}^{\alpha\beta}/p_B^\alpha)^3(p_{BA}^{\alpha\beta}/p_B^\alpha)$
2	2	0	$6p_B^\alpha (p_{BB}^{\alpha\beta}/p_B^\alpha)^2(p_{BA}^{\alpha\beta}/p_B^\alpha)^2$
3	1	2	$4p_B^\alpha (p_{BB}^{\alpha\beta}/p_B^\alpha)(p_{BA}^{\alpha\beta}/p_B^\alpha)^3$
4	0	4	$p_B^\alpha (p_{BA}^{\alpha\beta}/p_B^\alpha)^4$

Comparison with Onsager's exact solution for the two-dimensional case is in order. In Fig. 2 we show the SROP for $Z=4$ nearest neighbors as a function of τ. A fairly good agreement is found with the exact solution, especially in the paramagnetic phase. At the transition point there is a finite discontinuity of the slope; this produces a finite jump in the specific heat, a fact which is typical in effective-field theories.

When the magnetic field is turned on the variation of η is smooth and no discontinuity appears in the derivative. We show an example for the ferromagnetic case in Fig. 3 where the magnetization is also shown.

Once the statistical mechanics are solved through the use of relations (12) to (14) the probabilities of formation of the various clusters can be obtained. As an example we list in Table I all the possible clusters for $Z=4$ and their corresponding probabilities. The effective field produced by the nearest-neighbor shell at the central spin site is also shown. From these results the resonant amplitudes and frequencies can be straightforwardly calculated.

III. RESONANCE PHENOMENA

In studying resonances of clusters we have only considered spin-flip transitions of the central spin in a frozen environment. Thus the effective field in a given site is constant during the process. In the case $Z=4$ we have five such transitions, while for $Z=6$ we end up with seven lines. In order to describe the above mentioned phenomena we have devised a special notation for cluster configurations. Given a fixed state $K(K=A,B)$ at a central site of ν type $(\nu=\alpha,\beta)$, we denote by λ the configuration of the shell of nearest neighbors. Thus for $Z=4$ we have the following possibilities:

$$\lambda=(AAAA),(AAAB),(AABB),(ABBB),(BBBB) \tag{21}$$

which correspond to the five transitions mentioned above. The probability of formation of a certain cluster will be written as $p[\nu K\lambda]$. For $Z=4$ they are listed in the last column of Table I. The following properties are easily verified:

$$\sum_\lambda p[\nu K\lambda]=p_K^\nu \ , \tag{22}$$

$$\sum_K\sum_\lambda p[\nu K\lambda]=p_A^\nu+p_B^\nu=1 \ . \tag{23}$$

In addition, λ can be written as a set of two numbers λ_A and λ_B, which are the number of nearest neighbors in states A and B, respectively. We note that

$$\lambda_A+\lambda_B=Z \tag{24}$$

and

$$\lambda_A - \lambda_B = h_\lambda \ , \tag{25}$$

where h_λ is the effective field of configuration $\lambda = (\lambda_A \lambda_B)$ at the central site of the cluster. Values of h_λ are displayed in Table I for $Z = 4$. The total field present at the central site can be written as

$$-\frac{J}{|J|} h_\lambda + h \ , \tag{26}$$

while explicit expressions for the probabilities $p[\nu_K \lambda_A \lambda_B]$ are given by

$$p[\nu K \lambda_A \lambda_B] = \frac{Z!}{\lambda_A! \lambda_B!} \left(\frac{p_{AB}^{\nu\nu'}}{p_K^\nu} \right)^{\lambda_A} \left(\frac{p_{AB}^{\nu\nu'}}{p_K^\nu} \right)^{\lambda_B} p_K^\nu \ , \tag{27}$$

where ν and ν' are nearest neighbors. The energy of individual clusters, in units of $|J|$, is therefore given by

$$\epsilon_{\nu K \lambda} = \left(\frac{J}{|J|} h_\lambda - h \right) S_K \ , \tag{28}$$

where

$$S_K = \begin{cases} +1 & \text{if } K = A \\ -1 & \text{if } K = B. \end{cases} \tag{29}$$

The statistical average over all the configurations for a given ν site yields the following mean field:

$$\langle h \rangle_\nu \equiv \sum_K \sum_\lambda \left(-\frac{J}{|J|} h_\lambda + h \right) (e^{-\epsilon_{\nu K \lambda}/\tau}/Z) p[\nu K \lambda] \ , \tag{30}$$

where Z_ν is the partition function for the ν site

$$Z_\nu \equiv \sum_K \sum_\lambda e^{-\epsilon_{\nu K \lambda}/\tau} p[\nu K \lambda] \ . \tag{31}$$

The transitions considered here correspond to spin flips of individual spins in a given effective field. The latter effective field varies from cluster to cluster. Individual clusters will be observed if the meas-

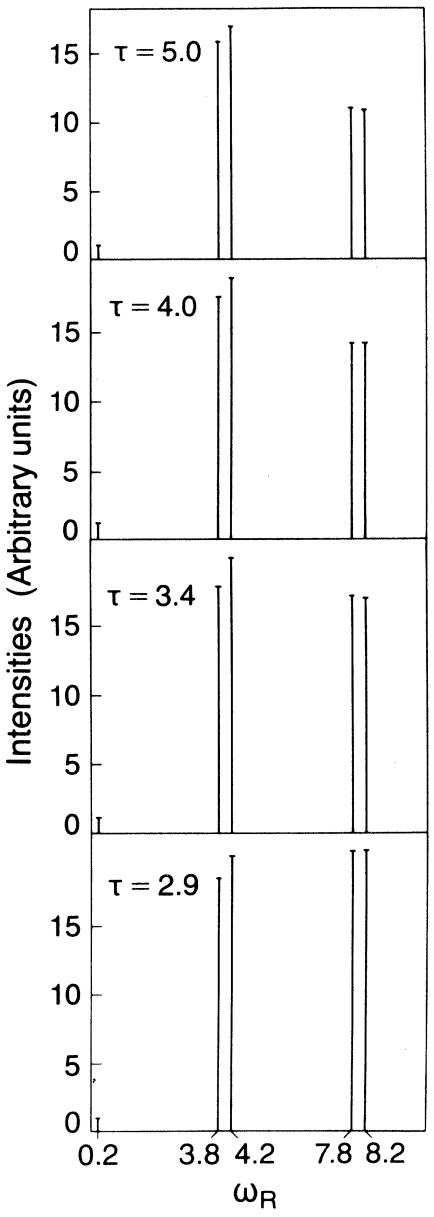

FIG. 4. Line intensities for spin-flip transitions in frozen cluster environments for different temperatures in the paramagnetic phase. The case depicted here corresponds to antiferromagnetic exchange ($J > 0$) for $Z = 4$ nearest neighbors, and the applied field in units of $|J|$ is taken as $h = 10^{-1}$. The resonance frequencies are indicated by arrows in the lowest part of the graph. An α site has been chosen, but no major differences appear for a β site in the paramagnetic region.

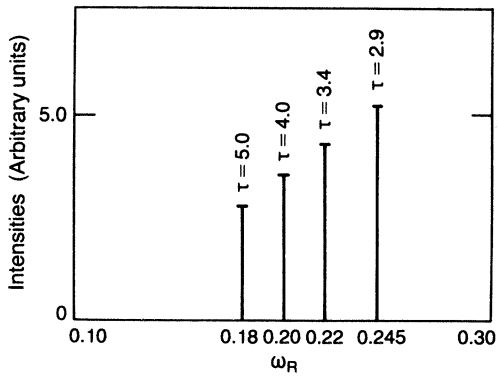

FIG. 5. Line intensities for spin-flip transitions in a mean effective field for different temperatures. The same cases shown in Fig. 4 are taken in order to make explicit the net shift of the effective field towards higher frequencies when the temperature is lowered. The temperature variation of the mean field is calculated through the use of relation (30) in the main text, where all the possible clusters have been superposed.

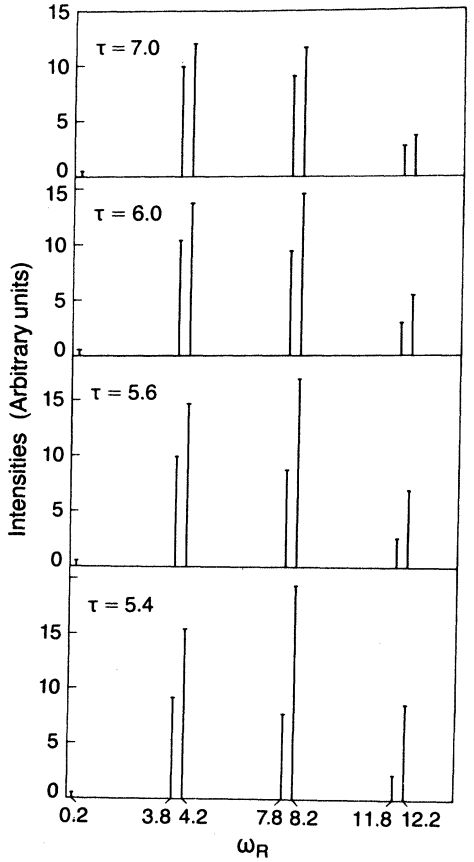

FIG. 6. This figure is similar to Fig. 4, now displaying the ferromagnetic case for $Z=6$ nearest neighbors. Seven lines, corresponding to spin-flip transitions in individual clusters, now appear. The applied magnetic field is $h=10^{-1}$. The critical temperature when no external field is present is given by formula (1) and turns out to be $\tau_c=4.93$. Observe that symmetry of line intensities is markedly broken well before the transition temperature. Clustering favors the situation of mean field $|h_\lambda|$ over its counterpart of mean field $-|h_\lambda|$. This effect is much weaker when we have antiferromagnetic exchange: The intensities of partner lines remain more or less the same in the paramagnetic phase (see Fig. 4 and Table II).

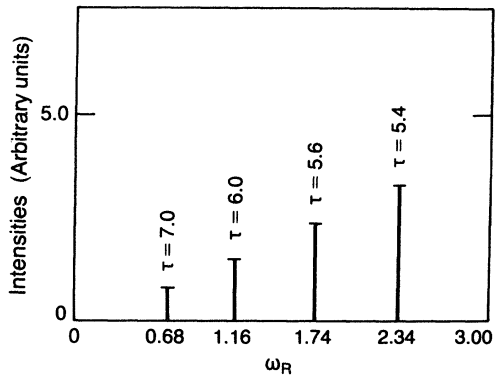

FIG. 7. The mean-field case corresponding to the situations shown in the preceding figure. The resonance shift is much larger now than in the antiferromagnetic case.

urement time is smaller than the characteristic decay time of fluctuations. Otherwise the resonant phenomenon will appear in terms of the mean effective field (30), where a weighted superposition of all possible clusters is made.

For single spin-flip transitions in a cluster of configuration λ the resonance frequency is given by

$$\omega_K^{\nu\lambda} \equiv 2\left|\frac{J}{|J|}h_\lambda - h\right| , \tag{32}$$

and the corresponding amplitude for the transition, in arbitrary units, is taken proportional to

$$I_{\nu\lambda} \equiv \frac{1}{Z_\nu}\left|e^{-\epsilon_{\nu K\lambda}/\tau}p[\nu K\lambda] - e^{-\epsilon_{\nu\bar{K}\lambda}/\tau}p[\nu\bar{K}\lambda]\right| , \tag{33}$$

where $\bar{K}$ means the spin state complementary to K,

$$p_{\bar{K}}^{\nu} \equiv 1 - p_K^{\nu} .$$

In Fig. 4 we show the different cluster lines for the antiferromagnetic case for $Z=4$. The temperature is lowered towards the Curie temperature. It can be verified, looking at Fig. 5, that there is a net shift of the mean effective field towards higher frequencies.

TABLE II. Line intensities for the different clusters as a function of temperature for the antiferromagnetic case and $Z=4$. The cases shown in Fig. 4 are also included for comparison purposes. The different lines are identified by their resonance frequencies. The transition temperature of this system (when no external field is applied) is $\tau_c=2.89$, and the magnetic field is $h=0.1$.

τ	$I(8.2)$	$I(7.8)$	$I(4.2)$	$I(3,8)$	$I(.2)$
5.0	10.8	10.9	16.8	15.7	1.1
4.0	13.9	14.1	18.8	17.5	1.2
3.4	16.9	17.0	19.8	18.3	1.1
2.9	20.3	20.3	20.0	18.4	1.1
2.8	50.2	4.0	25.3	6.5	0.7
2.4	81.4	0.1	15.2	0.3	0.5
2.0	93.9	0.0	5.5	0.1	0.0

TABLE III. Line intensities for two lines from Fig. 6 as a function of temperature. The lines are identified by their resonance frequency. The transition temperature of this system ($J>0$, $Z=6$) with no external field is $\tau_c=4.93$. Units are arbitrary but same normalization and same magnetic field as in Table II are used.

τ	$I(12.2)$	$I(8.2)$
7.0	3.9	11.7
6.0	5.5	14.6
5.6	7.1	17.1
5.4	8.7	19.4
5.0	19.5	29.4
4.94	23.2	31.3
4.4	51.9	32.5
4.0	68.8	24.9
3.4	85.9	12.8

The same phenomenon appears more markedly in Figs. 6 and 7 where we have depicted the ferromagnetic case for $Z=6$ nearest neighbors. Since our interest is primarily focused on the paramagnetic region we have not shown examples of resonant lines for temperatures corresponding to the ordered phase (ferro or antiferromagnetic). On physical grounds we expect saturation of the line of highest frequency (which corresponds to a spin-flip transition in a perfectly aligned ferromagnetic or antiferromagnetic cluster) along with a rapid decaying of all the other lines. In Tables II and III we show some values of line intensities for lower temperatures. The units are arbitrary but all the intensities are normalized to the same factor. Along with this process, we note that the resonant frequency of the mean situation (weighted average over cluster configurations) shifts to the position of the perfectly ordered cluster line when the temperature is lowered well into the ordered phase. This fact is shown in Tables IV and V for the two examples worked out here.

TABLE IV. The resonance frequency for a spin-flip transition in a mean effective field as a function of temperature. The case considered here corresponds to antiferromagnetism with $Z=4$ nearest neighbors. The applied field is $h=0.1$.

τ	ω_R
5.0	0.18
4.0	0.20
3.4	0.22
2.9	0.25
2.8	4.74
2.2	7.74
1.8	8.06

TABLE V. Resonance frequency for the average effective field spin-flip transition as function of temperature. This table corresponds to the ferromagnetic case with $Z=6$ nearest neighbors and the applied magnetic field is $h=0.1$. The critical temperature of this system (no external field) is $\tau_c=4.93$.

τ	ω_R
7.0	0.68
6.0	1.16
5.6	1.74
5.4	2.34
4.94	6.10
4.00	10.70
3.4	11.60

The important point we want to emphasize is that short-range order produces a net shift of the effective field even in the paramagnetic phase (see Figs. 5 and 7). This effect has been observed experimentally[7,8] and is absent in standard molecular-field theory.

IV. CONCLUSIONS

No satisfactory treatment of short-range order in critical phenomena is readily available. The renormalization-group approach[11] is well defined in the so-called critical region, where the scaling hypothesis is valid and where the behavior of the system is dominated by long-range fluctuations.

The method presented in this paper is an effective-field theory which improves the results of the classical Weiss molecular field by taking into account short-range order effects in the paramagnetic region. Poor results concerning critical exponents are therefore expected. However, for the disordered phase the model is in good agreement when compared with some exact solutions (see Fig. 2).

Concerning the ESR phenomena we may distinguish three important regions according to the temperature.

(A) For high temperatures $\tau=k_BT/|J|\gg 1$ no effective coupling among nearest neighbors can be detected. If the applied magnetic field is small (compared to $|J|$) for high temperatures in the paramagnetic phase we get

$$p_A^{\alpha}\approx p_B^{\alpha}\approx p_A^{\beta}\approx p_B^{\beta}\approx\frac{1}{2}$$

and

$$p_{AA}^{\alpha\beta}\approx p_{AB}^{\alpha\beta}\approx p_{BB}^{\alpha\beta}\approx p_{BA}^{\alpha\beta}\approx\frac{1}{4}\ .$$

So one cluster of effective field h_λ is as likely to occur as the other cluster with inverted effective field $(-h_\lambda)$. The net result for the average field given by expression (30) is

$$\langle h \rangle_\nu \approx h \ .$$

The short lifetimes of fluctuations for the different clusters are approximately the same, no long-range order is present ($M=0$) and no local effective field is developed (short-range order absent). The only transitions detected should correspond to spin-flip transitions in the applied field h (if detectable from the background of rapid thermal fluctuations).

(B) As the temperature is lowered towards the critical point, thermal fluctuations slow down and short-range order develops in the system inducing an effective local field. Up and down random orientations of clusters still yield $M \approx 0$ for each sublattice magnetization. The induced effective field produces a shift of the resonance frequency to higher fields as indicated by Figs. 5 and 7. Not all the fluctuations are equally long lived now and some of the cluster lines may appear in the form of a splitting of the spectrum (if enough resolution is available). This is the regime we are mainly interested to describe in order to make connection with experimental works.[7,8] Our predictions explain qualitatively the latter observations.

(C) For the critical region our model is not a good approximation as it has already been discussed. Moreover spin waves modes are absent in the Ising magnet (no transverse coupling of spins is included) and therefore our model should be looked at cautiously in the ordered phase. When approaching the critical region the dynamical character of the phenomenon is extremely important. Long-range and long-lived fluctuations (clusters of larger and larger size) develop which eventually encompass the whole system. The response is then mainly determined by those long-lived excitations; these decay infinitely slowly for wave vector $k \to 0$ (long-wavelength fluctuations), and arise spontaneously as a manifestation of symmetry breaking and long-range order.

As far as the paramagnetic phase is concerned our treatment is entirely satisfactory and extensions to other lattice structures (such as the triangular lattice and the fcc structure) are currently under study.

ACKNOWLEDGMENTS

One of us (G.G.C.) wants to acknowledge stimulating discussions with Dr. R. B. Stinchcombe at the ICTP (Trieste). Two of the authors (A.M.S. and G.G.C.) are grateful to CNPq (Brazil) for partial financial support. The work at the University of California, Berkeley (L.M.F.) was supported in part by the National Science Foundation through Grant No. DMR 78-03408.

APPENDIX: ISING FERROMAGNETIC CHAIN WITH EXTERNAL FIELD

This case can be calculated exactly using Eqs. (12) to (14) in the main text. With the reduced variables defined by Eqs. (19) and (20) we get

$$M = \frac{\sinh(h/\tau)}{[\cosh^2(h/\tau) - 2e^{-2/\tau}\sinh(2/\tau)]^{1/2}} \ , \qquad \text{(A1)}$$

for the magnetization. The short-range order parameter η is given by

$$\eta = 1 + \frac{2F^{1/2}}{G^2-1}\left[F^{1/2} - G\cosh\left[\frac{h}{\tau}\right]\right] \times \left[\frac{1-2G^{-1}\sinh 2/\tau}{M^2}\right]\sinh^2\left[\frac{h}{\tau}\right] \ , \qquad \text{(A2)}$$

where

$$F \equiv G^2\cosh^2(h/\tau) + (1-G^2) \ ,$$

$$G \equiv e^{2/\tau} \ .$$

[1] J. S. Smart, *Effective Field Theories of Magnetism* (Saunders, Philadelphia, 1966).
[2] G. G. Cabrera, Am. J. Phys. 46, 1062 (1978).
[3] R. Kikuchi, Phys. Rev. 81, 988 (1951).
[4] R. C. Kittler and L. M. Falicov, Phys. Rev. B 18, 2506 (1978).
[5] J. L. Morán-López and L. M. Falicov, Phys. Rev. B 18, 2542, 2555 (1978).
[6] A. Stein and G. G. Cabrera (unpublished).
[7] J. F. Suassuna, C. Rettori, H. Vargas, G. E. Barberis, and C. E. Hennies, J. Phys. Chem. Solids 38, 1075 (1977).
[8] C. Rettori, G. E. Barberis, and J. F. Suassuna (private communication).
[9] See, for instance, D. C. Mattis, *The Theory of Magnetism* (Harper and Row, New York, 1965), Chap. 9.
[10] C. Domb, Adv. Phys. 9, 245 (1960).
[11] S. K. Ma, *Modern Theory of Critical Phenomena* (Benjamin, Reading, Mass., 1976).